Tikrit Journal of Engineering Sciences (2025); 32(3): 2346
DOI: http://doi.org/10.25130/tjes.32.3.27

IRAQI Academic Scientific Journals

ISSN: 1813-162X (Print); 2312-7589 (Online)
Tikrit Journal of Engineering Sciences
available online at: http://www.tj-es.com

TJES Tikrit Journal of Engineering Sciences

Modeling and Analysis of Quasi-Z Source IMC Converter Feeding PMSM Drive System

H. A. Hasan [a], *Ahmed K. Hannan* [*a], *Waleed M. Zapar* [b], *Ezzulddin Ahmed* [c], *Abdelrahman Farghly* [d]
a Council Affairs, University of Baghdad, Baghdad, Iraq.
b Service and Maintenance, University of Anbar, Anbar, Iraq.
c Department of Electrical Engineering, College of Engineering, University of Baghdad, Iraq.
d Department of Electrical Engineering, College of Engineering, University of Alexandria, Egypt.

Keywords:
Field-oriented control; Indirect matrix converter; Permeant magnet synchronous machine (PMSM); Quasi-Z-Source; Space Vector PWM; Shoot-Through Duty Ratio; Voltage Gain.

Highlights:
- *Increase the voltage gain for a quasi-Z-source indirect matrix converter (IMC).*
- *Drive PMSM with a wide speed range drive system using SVPWM with low THD.*
- *Filter the input current and increase the power factor.*

ARTICLE INFO
Article history:

Received	16 Sep. 2024
Received in revised form	19 Sep. 2024
Accepted	30 Sep. 2024
Final Proofreading	25 Aug. 2025
Available online	28 Aug. 2025

Citation: Hannan AK, Hasan HA, Zapar WM, Ahmed E, Farghly A. **Modeling and Analysis of Quasi-Z Source IMC Converter Feeding PMSM Drive System**. *Tikrit Journal of Engineering Sciences* 2025; **32**(3): 2346.
http://doi.org/10.25130/tjes.32.3.27

***Corresponding author:**
Ahmed K. Hannan
Council Affairs, University of Baghdad, Baghdad, Iraq.

Abstract: The purpose of this study is to increase the voltage gain (U_g) for a quasi-Z-source indirect matrix converter (IMC) feeding a three-phase Permanent Magnet Synchronous machine (PMSM) drive system. Due to the low U_g of the IMC, a quasi-Z-source development was connected with the traditional IMC to boost the motor's supply voltage. Space Vector modulation (SVPWM) was used to generate the required switching signals (PWM) for the proposed converter. The system U_g increased as a result of the shoot-through duty (D) of the rectifier side, which increases the output voltage amplitude for the quasi-Z-source system. The proposed converter can regulate the output voltage of quasi-Z-source IMC automatically under voltage sag, step changes in applied load torque on the motor, and changes in the desired speed when the required U_g of quasi-Z-source IMC is greater than 0.866. This value is achieved by choosing the optimized value of D and the modulation index of the rectifier side (m_o). Variable speed from zero to the rated value can be controlled by using closed-loop field-oriented control. The proposed converter was simulated in the MATLAB/Simulink environment to verify the system's efficiency.

نمذجة وتحليل محول مصفوفة غير مباشر ذو مصدر شبّه الممانعة يغذي محرك متزامنً دائم المغناطيس

حسن علي حسن[1] ، احمد كامل حنان[1]، وليد م. زبار[2]، عزالدين احمد[3]، عبدالرحمن فرغلي[4]
[1] شؤون المجلس/ جامعة بغداد/ بغداد – العراق.
[2] قسم الخدمة والصيانة/ جامعة الأنبار/ الأنبار – العراق.
[3] قسم الهندسة الكهربائية/ كلية الهندسة/ جامعة بغداد – العراق.
[4] قسم الهندسة الكهربائية/ كلية الهندسة/ جامعة الإسكندرية/ مصر.

الخلاصة

الغرض من هذه الدراسة هو زيادة كسب الجهد (U_g) لمحول مصفوفة غير مباشر (IMC) شبه مصدر Z يغذي نظام محرك آلة متزامنة مغناطيسية دائمة ثلاثية الطور (PMSM). نظرًا لانخفاض U_g لـ IMC، يتم توصيل مصدر شبه Z للتطوير مع IMC التقليدي لتعزيز جهد الإمداد للمحرك. يتم استخدام تعديل متجه الفضاء (SVPWM) لتوليد إشارات التبديل المطلوبة (PWM) للمحول المقترح. يزداد نظام U_g نتيجة لواجب الإطلاق (D) لجانب المقوم، مما يزيد من سعة جهد الخرج لنظام المصدر شبه Z. يمكن للمحول المقترح تنظيم جهد الخرج لـ IMC شبه المصدر Z تلقائيًا تحت انخفاض الجهد، والتغيرات التدريجية في عزم الحمل المطبق على المحرك، والتغيرات في السرعة المطلوبة عندما تكون U_g المطلوبة لـ IMC شبه المصدر Z أكبر من 0.866، ويتم تحقيق ذلك عن طريق اختيار القيمة المثلى لـ D ومؤشر التعديل لجانب المقوم (m_o). يمكن التحكم في السرعة المتغيرة من الصفر إلى القيمة المقدرة باستخدام التحكم الموجه نحو المجال في الحلقة المغلقة. يتم محاكاة المحول المقترح في بيئة MATLAB / Simulink للتحقق من كفاءة النظام.

الكلمات الدالة: التحكم الموجه نحو المجال، محول مصفوفة غير مباشر، محرك ذات مغناطيس نافذ (PMSM)، مصدر شبه Z، متجه فضائي مولد PWM، نسبة واجب الإطلاق، كسب الجهد.

1.INTRODUCTION

The most common use of AC-AC converter topologies in industrial applications is a conventional DC-bus voltage source converter. DC-bus capacitor makes the conventional back-to-back bulky and reduces its operational lifespan [1-3]. Gyugi and Pelly developed the AC-AC converter without a DC link capacitor component and with a forced commutated Cyclo-converter [4, 5]. The matrix converter (MC) configurations are categorized into direct matrix converter (DMC) and indirect matrix converter (IMC). The IMC overcomes the commutation challenges associated with the DMC [6-8]. Both have been key research areas for many years. Compared to the Back to Back converter (B2BC), the matrix converter stands out because of its most impressive features, such as its unity power factor, high power density, low harmonics with sinusoidal waveforms, bidirectional power flow, reliability, and extended lifetime in hostile situations, make the matrix converter most impressive [9, 10]. The IMC performs two stages (AC-DC-AC) conversions without a DC-bus capacitor filter, while DMC only does a single stage (AC-AC) conversion. Both converters share the same features; the IMC's simple commutation is more akin to the B2BC's than the DMC's [11]. Despite several features in the development of the MC, its limitations have prevented it from becoming widely used in industry [12]. Similar to B2BC, MC's voltage transfer ratio of 0.866 is relatively low. Many studies were conducted to improve the voltage ratio, which connects a transformer in series with the input supply voltages and the load. However, a bulky transformer also affects the MC's compactness. Over-modulation region operation of the MC is another way [13]. After that, a Z-source IMC was proposed to increase the DC-bus voltage of the inverter by adding the Z-source network between the rectifier side and inverter side of the IMC [14]. However, in this case, the DC-bus requires sizable capacitors and inductors [15, 16]. To improve voltage gain with fewer switches and passive components, a specific type of Z-source DMC was proposed. However, they still have to resolve the DMC's difficult commutation. In the present paper, quasi-Z-source IMC is used to feed the synchronous machine drive system under supply voltage sag. Closed-loop field-oriented control is used to get accurate speed control with a variable load. Space vector modulation (SVPWM) is used to generate the required switching signals. The present paper is divided into the following sections: In Section 2, the proposed quasi-Z-Source IMC is introduced with SVPWM. Section 3 presents the analysis and operation of the quasi-Z-Source IMC. Section 4 presents the parameter design of the quasi-Z-source and the algorithm of the shoot-through duty ratio. Section 4 presents the field-oriented control strategy. Finally, Section 5 presents the simulation results.

2.THE PROPOSED QUASSI-Z-SOURCE IMC

The proposed quasi-Z-source IMC converter, as shown in Fig. 1, contains three parts: the quasi-Z-source, the rectifier side, and the inverter side. The quasi-Z-source is added with the supply voltage, and it consists of three switches, S_j (j= a, b, and c), that can be controlled by the required switching signals (PWM), and six capacitors C_{jz}, and inductors L_{jz} (z= 1, 2, and 3). The proposed converter can operate in the buck and boost modes because it has the same switching signal PWM due to a special impedance network [17].

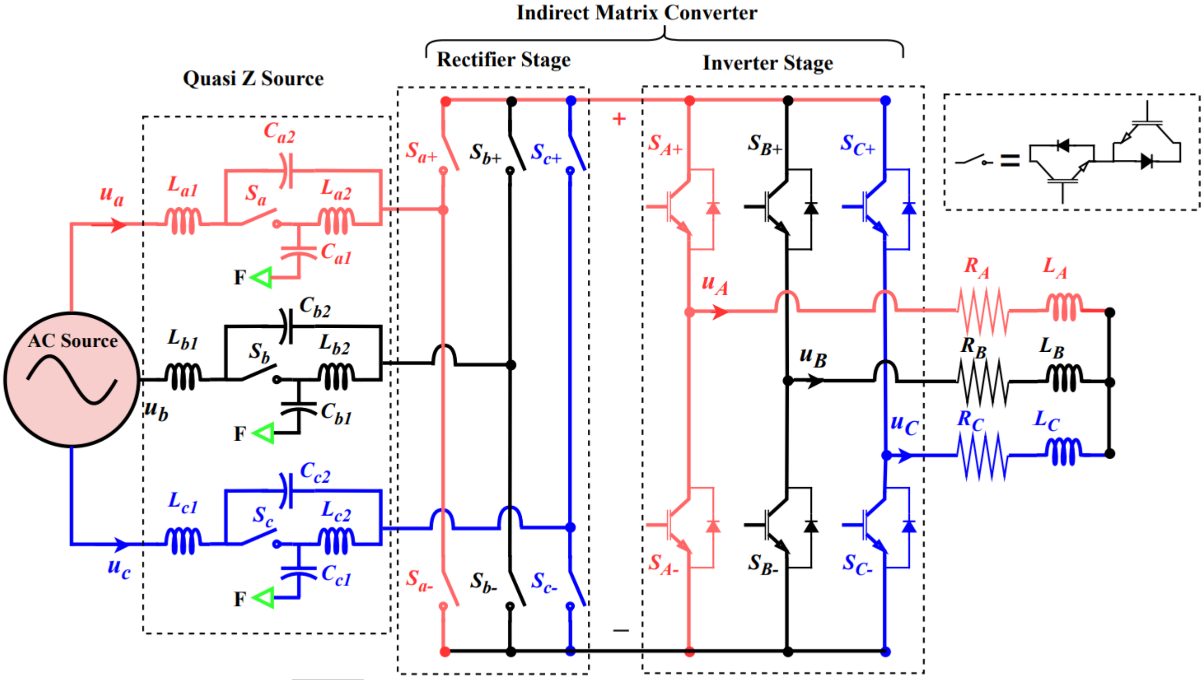

Fig. 1 The Proposed Quasi-Z-Source IMC Converter.

2.1.Space Vector Modulation for IMC (SVPWM)

Space vector modulation is an alternate approach to operating PWM switches that focuses on efficiency, user-friendliness, reducing the total harmonic distortion (THD), and optimizing the transfer ratio. The SVM algorithm claims many advantages. These characteristics render SVPWM more suitable for applications that need high voltage, as the complexity of states and the number of redundant switching states show a substantial increase with the number of levels. The SVPWM is employed to ensure that the output voltages of the inverter match the correct values at any switching time with a smaller time delay [18]. SVPWM is a power electronic switching control technology that recognizes switching sequences by assigning a switching vector in the *d-q* space [19-21]. By selecting the valid switching States of a three-phase matrix converter and determining their corresponding on-time duration, the SVPWM approach is utilized to regulate the voltage and frequency of the inverter stage [22]. For the rectifier stage, the supply current is fed to the SVPWM to generate the desired sinusoidal input current and is controlled by the power factor. The modes of the rectifier's switches are classified as active vectors or zero vectors. To increase the output voltage of the quasi-Z-source by inserting the shoot-through zero vector during the zero vector of the rectifier stage, a simple boost control was presented in [23, 24], as shown in Table 1. In this condition, a voltage boost is obtained by short-circuiting the three-phase supply voltage [25, 26]. For example, select sector one, the vectors I_{ab} and I_{ac} combine to generate the input reference current vector, I_{ref}, as shown in Fig. 2.

Table 1 DC-Bus Voltage, Switching Groups, and Input Current Vectors.

N	U_{dc}	S_{a+}	S_{b+}	S_{c+}	S_{a-}	S_{b-}	S_{c-}	Vector	State
1	U_{ac}	1	0	0	0	0	1	I_{ac}	Active
2	U_{bc}	0	1	0	0	0	1	I_{bc}	Active
3	$-U_{ab}$	0	1	0	1	0	0	$-I_{ab}$	Active
4	$-U_{ac}$	0	0	1	1	0	0	$-I_{ac}$	Active
5	$-U_{bc}$	0	0	1	0	1	0	$-I_{bc}$	Active
6	U_{ab}	1	0	0	0	1	0	I_{ab}	Active
7	zero	1	0	0	1	0	0	I_{aa}	Zero
8	zero	0	1	0	0	1	0	I_{bb}	Zero
9	zero	0	0	1	0	0	1	I_{cc}	Zero
10	zero	1	1	1	0	0	0	I_d	Shoot-through zero vector
11	zero	0	0	0	1	1	1	I_d	Shoot-through zero vector

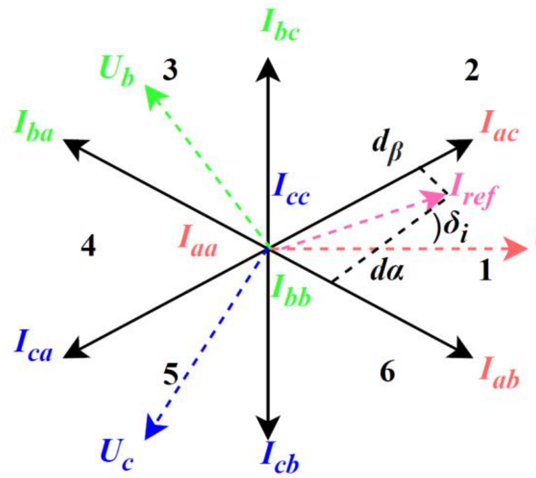

Fig. 2 SVPWM for Rectifier Side.

From the three vectors in the sector, the duty cycles can be obtained by:

$$d_\alpha = m_{in} \sin\left(\frac{\pi}{6} - \delta_i\right) \quad (1)$$

$$d_\beta = m_{in} \sin\left(\delta_i + \frac{\pi}{6}\right) \quad (2)$$

$$d_s = Const(d_S \leq 1 - d_\alpha - d_B) \quad (3)$$

$$d_{Or} = 1 - d_\alpha - d_\beta - d_S \quad (4)$$

where ($m_{in} = 1 - D$) is the modulation index of the rectifier side, δ_i is the input current vector angle, and d_α, d_β, d_s, and d_{Or} are the duty ratios of active vectors, shoot-through, and zero vectors, respectively. Figure 3 shows the SVPWM diagram for the inverter side.

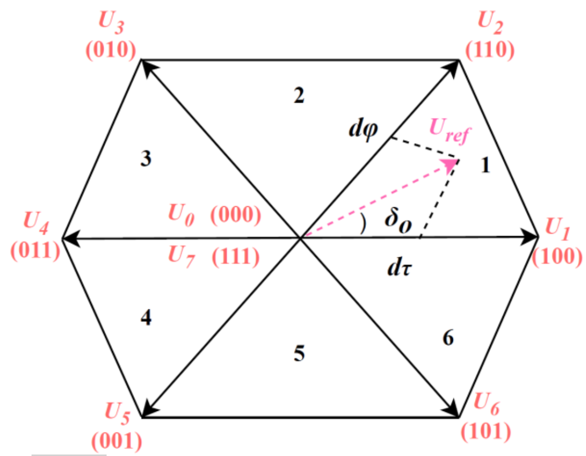

Fig. 3 SVPWM Diagram of the Inverter Side.

The inverter side is similar to a conventional voltage source inverter, which contains six effective vectors and two zero vectors [27]. The duty ratios can be obtained by:

$$d_\tau = m_{out} \sin\left(\frac{\pi}{3} - \delta_i\right) \quad (5)$$

$$d_\varphi = m_{out} \sin \delta_0 \quad (6)$$

$$d_{oi} = 1 - d_\tau - d_\varphi \quad (7)$$

where m_{out} is the modulation index of the inverter side, δ_0 is the output voltage vector angle, and d_τ, d_φ, and d_{oi} are the duty ratios of active vectors and zero vectors, respectively. The modulation pattern combines the switching states of two stages in one switching period to provide a balance of the supply input currents and the output voltages. Because the DC-bus has two positive line-to-line input voltages, the inverter stage-switching pattern must be divided into two groups. The resulting switching sequence is shown in Fig. 4. Duty cycles can be determined using the following formulas:

$$d_{u\alpha} = d_u \cdot d_\alpha \quad (8)$$

$$d_{u\beta} = d_u \cdot d_\beta \quad (9)$$

$$d_{v\alpha} = d_v \cdot d_\alpha \quad (10)$$

$$d_{oi\alpha} = d_{oi} \cdot d_\alpha \quad (11)$$

$$d_{oi\beta} = d_{oi} \cdot d_\beta \quad (12)$$

where $d_{u\alpha}$, $d_{u\beta}$, $d_{v\alpha}$, $d_{u\alpha}$, $d_{oi\alpha}$, and $d_{oi\beta}$ are the duty cycles of different vectors of output voltage for one switching period. Figure 4 shows that during commutation in the rectifier stage, the DC bus current is zero, and the inverter operates on a zero vector. As a result, during commutation, zero current switching is ensured on the rectifier stage, reducing switching losses and simplifying the commutating problem, which is quite complex with DMC [28].

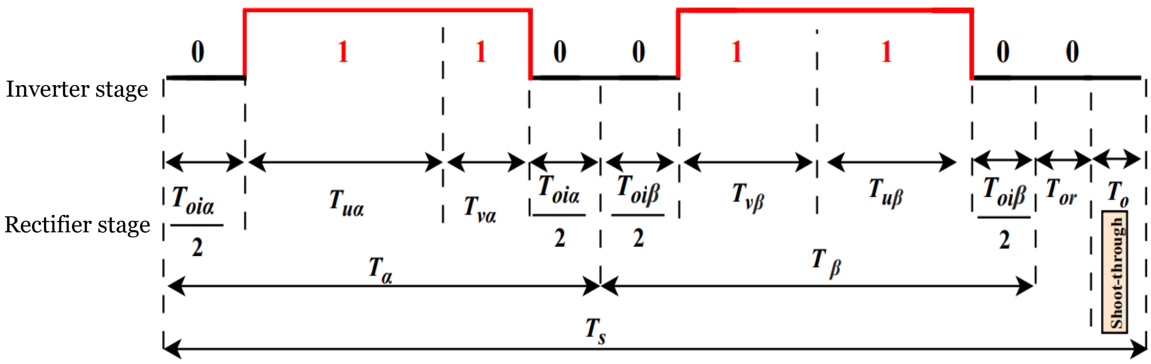

Fig. 4 Switching Sequences for the Proposed Converter.

2.2. Operation and Analysis of the Proposed Converter

The proposed converter is operated in two states called the shoot-through state and non-shoot-through state, as shown in Fig. 5. In the shoot-through state, the switch of the upper side of the rectifier, which is marked green color S_{j+} (j= a, b, and c), is switched on (short circuit). The switches S_j of the quasi-Z-source are switched off (open circuit), as shown in Fig. 5 (a). In this case, the arm inductors of the quasi-Z-source will charge for one switching time. The shoot-through duty cycle can be obtained ($D = T_o/T_s$). Thus, by adjusting the shoot-through duty, the output voltages of the quasi-Z-source can be increased to the desired value.

Since $L = L_{jz}$, and C=C_{ji}, j (a, b, c), z (1, 2, 3) from Fig. 5 (a), the following equations can be obtained:

$$u_{Lj1} = u_j + u_{cj2} - R_L \times i_{Lj1} \quad (13)$$

$$u_{Lj2} = u_{cj1} - R_L \times i_{Lj2} \quad (14)$$

$$i_{C_{j1}} = -i_{L_{j2}} \quad (15)$$

$$i_{C_{j2}} = -i_{L_{j2}} \quad (16)$$

In the non-shoot-through state, as shown in Fig. 5 (b), the three bidirectional switches S_j of the quasi-Z-source are switched on (short circuit), which is marked green, with a time period *(1-D) Ts*, and the switch of the upper side of the rectifier operates conventionally. In this case, the Inductors charge the capacitors, and the output voltages of the quasi-Z-source are the summation of the voltage across the two capacitors in each phase [13].

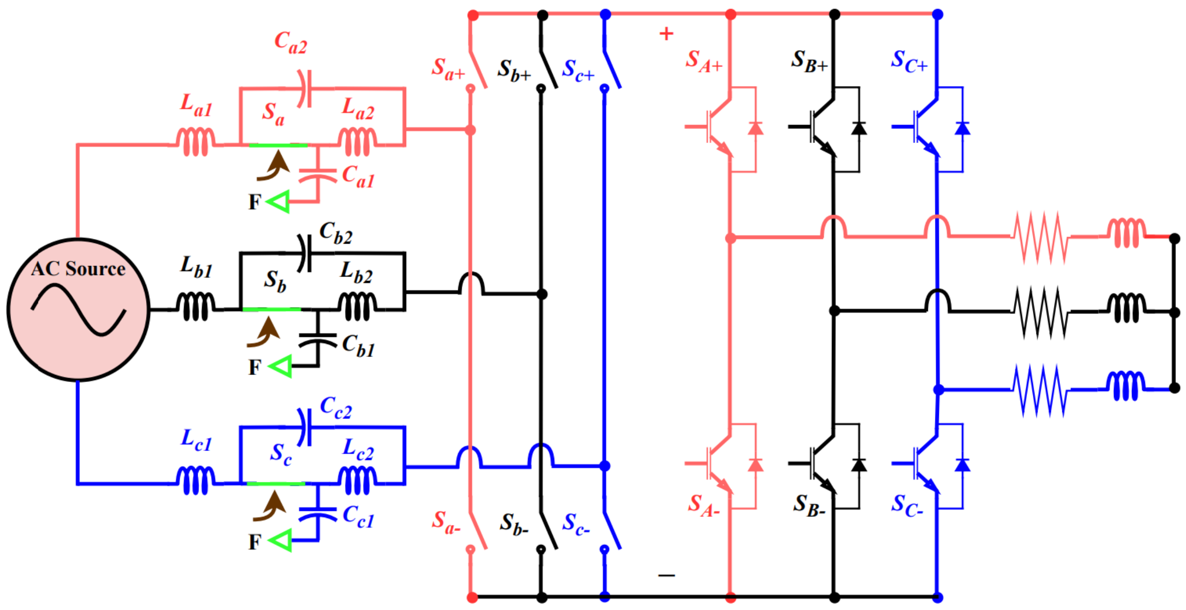

(a)

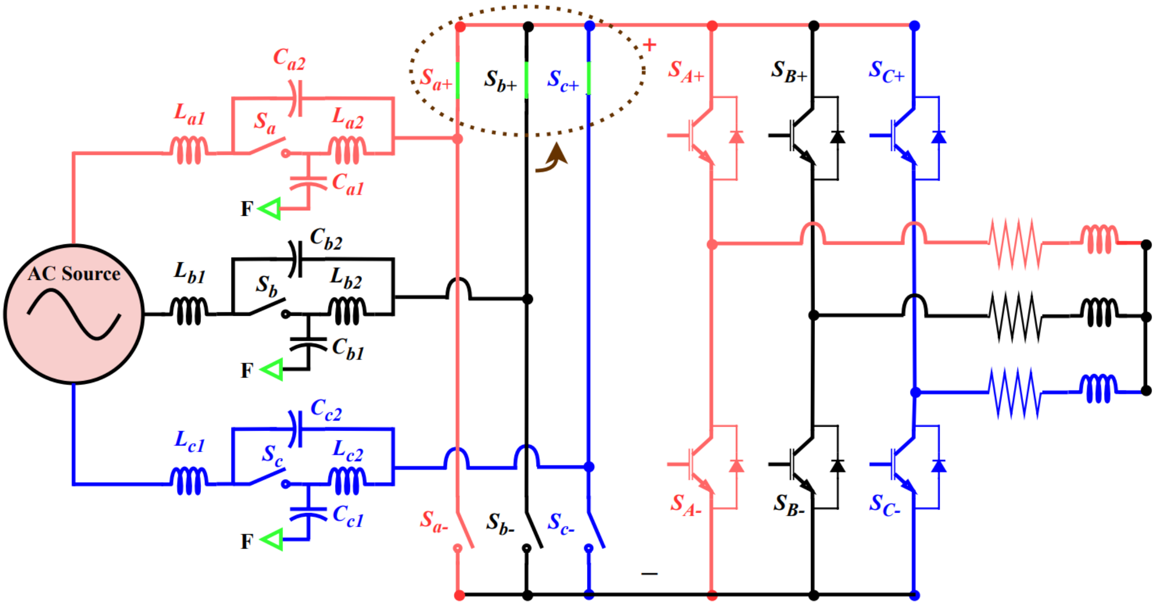

(b)

Fig. 5 The Proposed Converter with: (a) Shoot-Through State, (b) Non-Shoot-Through State.

From Fig. 5 (b), the following equations can be obtained:

$$u_{L_{j1}} = u_j - u_{c_{j1}} - R_L \times i_{Lj1} \quad (17)$$

$$u_{L_{j2}} = -u_{c_{j2}} - R_L \times i_{Lj2} \quad (18)$$

$$i_{C_{j1}} = i_{L_{j2}} - i'_j \quad (19)$$

$$i_{C_{j2}} = i_{L_{j2}} - i'_j \quad (20)$$

where u'_j, and i'_j are the output voltages and currents of the quasi-Z-source, respectively. For one sampling time T_s, the average voltage across the quasi-Z-source inductors and the average current through the quasi-Z-source capacitors should be zero, $R_L = 0$. Therefore, Eqs. (13)-(20), the average equations can be written as:

$$u_{L_{j1}} = D\left(u_j + u_{c_{j2}}\right) + (1-D)\left(u_j - u_{c_{j1}}\right) = 0 \quad (21)$$

$$u_{L_{j2}} = D\left(u_{c_{j1}}\right) + (1-D)\left(-u_{c_{j2}}\right) = 0 \quad (22)$$

$$i_{C_{j1}} = D\left(i_{L_{j2}}\right) + (1-D)\left(i_{c_{j1}} - i'_j\right) = 0 \quad (23)$$

$$i_{C_{j2}} = D\left(-i_{L_{j1}}\right) + (1-D)\left(i_{L_{j2}} - i'_j\right) = 0 \quad (24)$$

where $i_{L_{ji}}$ is the inductor current. From Eqs. (21)-(24), the capacitor voltages and the current that pass through the inductors of the quasi-Z-source are:

$$u_{c_{j1}} = \frac{(1-D)}{(1-2D)} u_j \quad (25)$$

$$u_{c_{j2}} = \frac{D}{(1-2D)} u_j \quad (26)$$

$$i_{L_{j1}} = i_{L_{j2}} = i_j \quad (27)$$

From Eqs. (25)-(27), the quasi-Z-source output voltages and currents can be written as:

$$u'_j = \frac{1}{1-2D} u_j \quad (28)$$

$$i'_j = \frac{(1-2D)}{(1-D)} i_j \quad (29)$$

As a result, the voltage boost factor (Q) can be written as:

$$Q = \frac{1}{1-2D} \text{ (If D < 0.5)} \quad (30)$$

The average DC-bus voltage of the proposed converter is:

$$U'_{dc} = \frac{3}{2} U_i \, Q \, m_{in} \cos(\theta_o) \quad (31)$$

where θ_o is the phase angle between the output phase voltage and the current of the quasi-Z-source. The modulation index m_{out} of the inverter side and the voltage gain U_g can be written as:

$$m_{\text{out}} = \frac{\sqrt{3}\, U_o}{U'_{dc}} \quad (32)$$

$$U_g = \frac{0.866(1-D)\, m_{\text{out}}}{1-2D} \quad (33)$$

3.CONTROL SHOOT-THROUGH DUTY RATIO

According to Eq. (33), to get the best choice of shoot-through duty ratio D, assume $m_{\text{out}} = 1$. Therefore, the shoot-through duty ratio can be expressed as:

$$D = \frac{U_0 - 0.866\, U_i}{2\, U_0 - 0.866\, U_i} \quad (34)$$

Figure 6 shows the control algorithm of the shoot-through duty ratio D. In the first stage, the amplitude of the input voltage and output voltage of the proposed converter is measured to obtain the voltage gain. In the second stage, the voltage gain is compared with the 0.886 factor to decide the operation of the proposed converter. If the voltage gain is equal to or less than 0.886. Then, the IMC does not need to increase the voltage, and the quasi-Z-source is operated as a filter with $m_{\text{in}} = 1$, and $D = 0$. On the other hand, when the voltage exceeds 0.866, the duty ratio will equal Eq. (34) to achieve optimal operation of the proposed converter.

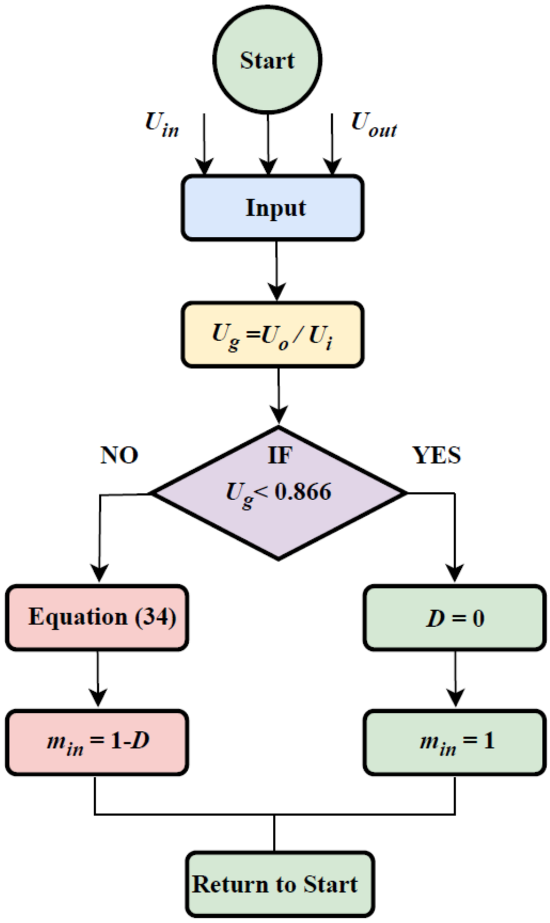

Fig. 6 Control Algorithm of the Duty Ratio.

4.PARAMETERS SELECTION OF QUASI-Z-SOURCE

Since the inductor of the quasi-Z-source is necessary to reduce the switching current fluctuation and the capacitor requires limiting switching voltage fluctuation, from shoot-through to non-shoot-through states, the voltage and current fluctuations are represented by the following expressions [29]:

$$\Delta \dot{i}_L = \frac{u_{jz} D(1-D)}{(1-2D)\,L} T_s \tag{35}$$

$$\Delta u_C = \frac{i_{Lj} D}{C} T_s \tag{36}$$

The inductance and capacitance of the quasi-Z-source can be calculated as [30]:

$$C \geq \frac{Iin_{\,rated}}{f_s k_u U_S}(1-2D) \tag{37}$$

$$L \geq \frac{U_i D(1-D)}{f_s\, k_i\, I_{rated}\,(1-2D)} \tag{38}$$

where $Iin_{\,rated}$ is the supply input current, f_s is the carrier frequency, and k_u and k_i represent the fluctuation ratio of the voltage and current, respectively.

5.FIELD ORIENTED CONTROL (FOC)

Field-oriented control (FOC) is a high-performance technique used to control synchronous and asynchronous machines, which is similar to the separately excited DC-machines speed control method [31, 32]. In recent years, FOC has become a widely accepted technique for AC motor drive systems [33-35]. FOC provides excellent control capability over the applied load torque and variable speed ranges. The FOC requires a transformation of stator currents from the stationary reference frame to the rotor flux reference frame (also called Clark-Park transformation) to obtain the direct current i_d and the quadrature current i_q [36]. The i_{ds} and i_{qs} can be calculated from the following expression:

$$\begin{bmatrix} i_d \\ i_q \end{bmatrix} = \frac{2}{3}\begin{bmatrix} \cos\theta_e & \cos(\theta_e - \partial) & \cos(\theta_e - 2\partial) \\ -\sin\theta_e & -\sin(\theta_e - \partial) & -\sin(\theta_e - 2\partial) \end{bmatrix}\begin{bmatrix} i_{A\,out} \\ i_{B\,out} \\ i_{C\,out} \end{bmatrix} \tag{39}$$

where θ_e represents the rotor angle, and $\partial = 2\pi/3$. For surface-mounted PMSM, the inductances L_d and L_q are equal, so the generated torque can be written as:

$$T_e = \frac{3}{2}\frac{p}{2}(\lambda_m \cdot i_q) \tag{40}$$

where p is the number of pole pairs, and λ_m is the permanent magnet flux linkage. The mechanical load torque and the rotor mechanical speed ω_r can be written as:

$$T_e = T_L + B \cdot \omega_r + J \cdot \frac{d\omega_r}{dt} \tag{41}$$

$$\omega_r = \int \left(\frac{T_e - T_L - B \cdot \omega_r}{J}\right) \cdot dt \quad (42)$$

where T_L is the applied load torque on the motor, J is the inertia coefficient, and B is the friction coefficient. Figure 7 shows the implementation of FOC. The motor speed is compared with the reference speed, and the error is applied to the PI controller to obtain i_q^*, which is proportional to the torque. Since the surface-mounted PMSM, the i_d^* is set to zero. After that, i_q^* and i_d^* are compared with actual i_q and i_d, and the error is applied to the PI controller to get u_d and u_q. At high speeds, to remove the coupling terms of u_q and u_q $((\omega_e(L_d i_d + \lambda_m)$ and $-\omega_e L_q\, i_q))$, a decoupling control block is used to remove the coupling part. u_q^{**} and u_d^{**} result from decoupling control block, and they are written as:

$$u_d^{**} = -\omega_e L_q\, i_q \quad (43)$$

$$u_q^{**} = \omega_e\,(L_d i_d + \lambda_m) \quad (44)$$

where $\omega_e = \frac{\omega_r\, p}{2}$ is the electrical rotor speed in rad/s. Finally, the references u_d^* and u_q^* are converted into (u_a^*, u_b^*, u_c^*) using inverse Park-Clark transformation [36].

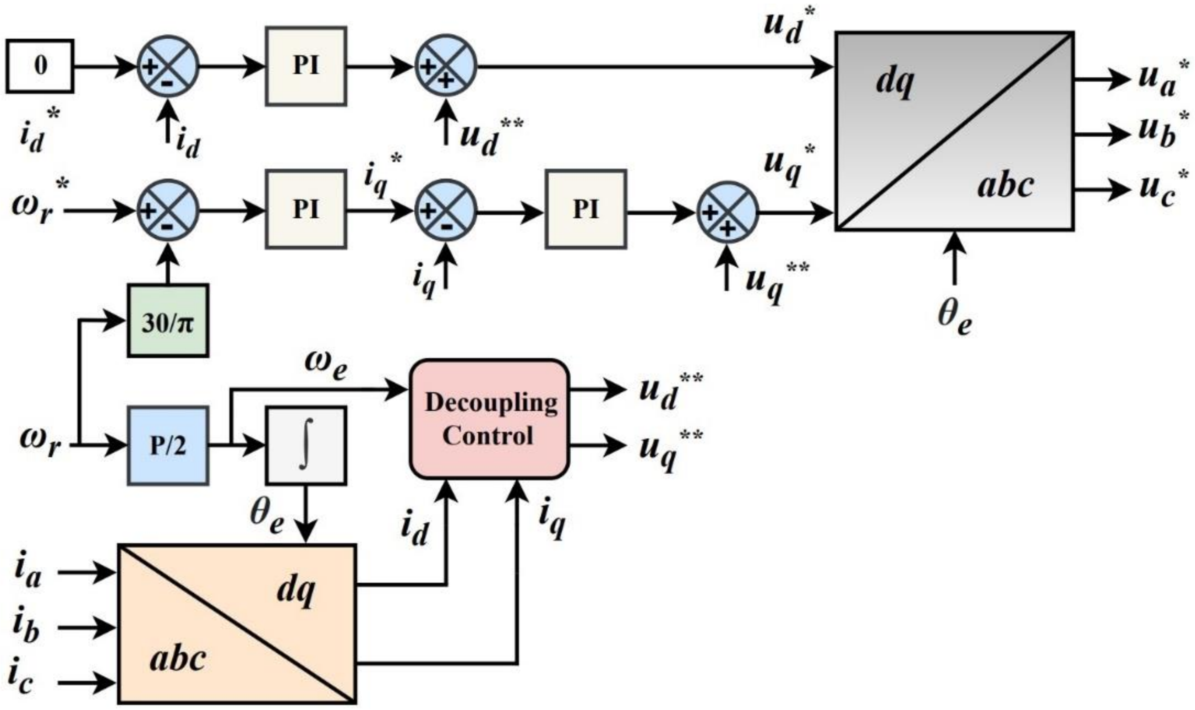

Fig. 7 FOC of PMSM.

6.PROPOSED CONVERTER BASED ON PMSM DRIVE SYSTEM

Figure 8 shows the proposed converter-fed PMSM. The quasi-Z-source supplies the inverter stage. The inverter stage feeds the PMSM with variable frequency and voltage, FOC to get the desired speed, and SVPWM to generate the required switching signals for the rectifier and inverter stages.

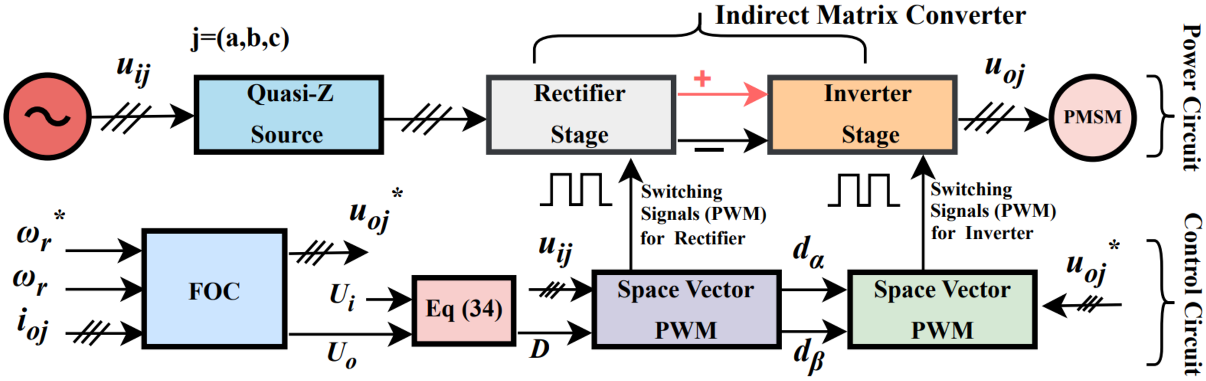

Fig. 8 The Proposed Converter Based on the PMSM Drive System.

7.SIMULATION RESULTS AND DISCUSSION

To evaluate the effectiveness of the proposed converter, the MATLAB\Simulink environment was used. The parameters of the drive system are listed in Table 2. The proposed converter was tested under two states to demonstrate its performance, i.e., transient and steady-state.

Table 2 Simulation Parameters.

Propused Converter Parameters	
Parameters	**Value**
Supply voltage U_{in}	220V/50Hz
DC-bus voltage U_{dc}	220V
Capacitance of quasi-Z-source C_1	10 µF
Capacitance of quasi-Z-source C_2	25 µF
Inductance of quasi-Z-source	4mH
Carrier frequency f_s	10kHz
PMSM Parameters	
Parameters	**Value**
Rated active power P_s	1.5 hp
Number of pole pairs pp	2
Rated speed	3000 rpm
Rated line-to-line voltage U_{rated}	380V
Rated load torque	3 N·m
Stator resistance	2.564 Ω
Stator inductance	8.5mH
Magnetic flux	0.172Wb
Moment of Inertia J	0.0008 kg-m²

7.1.State 1

In this state, the PMSM was operated with variable speeds, i.e., 500, 1500, 2500, and 3000 rpm, with a load torque of 2 N·m from 0 to 5.5 seconds. After each 1.5 second, the speed increased, as shown in Fig. 9. At 5.5 second, the applied load torque increased with its rated value, as shown in Fig. 10. Also, the quadrature current i_q increased because it is proportional to the torque, as shown in Fig. 11. The motor speed remained at the same value 3000 rpm because the PI controller returned it to the set value. As the applied load torque increased, the output currents also increased with THD, i.e., 1.85 %, 2.5%, 2.91%, and 3.12%, respectively, as shown in Fig. 12. The torque increased with the speed, according to Eq. (41). The supply input current increased due to the increase in the output currents with THD, i.e., 2.12%, 2.35%, 2.6% and 3.4%, as shown in Fig. 13. From (0-1500) rpm, there is no need to increase the voltage because the voltage gain U_g is less than 0.866. Thus, the shoot-through duty ratio was 0, and the quasi-Z-source operated as a filter. However, when the speed exceeded 1500 rpm, the shoot-through duty ratio D also increased. This behavior occurred because the quasi-Z-source's voltage gain exceeded that of the conventional IMC, with U_g > 0.866, which is determined by the required speed. Increasing the load torque at 5.5 seconds increased the duty ratio D, as shown in Figs. 14 and 15, respectively. The converter output voltages were regulated to obtain the required motor speed and load, as shown in Fig. 16. The DC-bus voltage increased as the output voltage increased to fit the desired output voltage, as shown in Fig. 17.

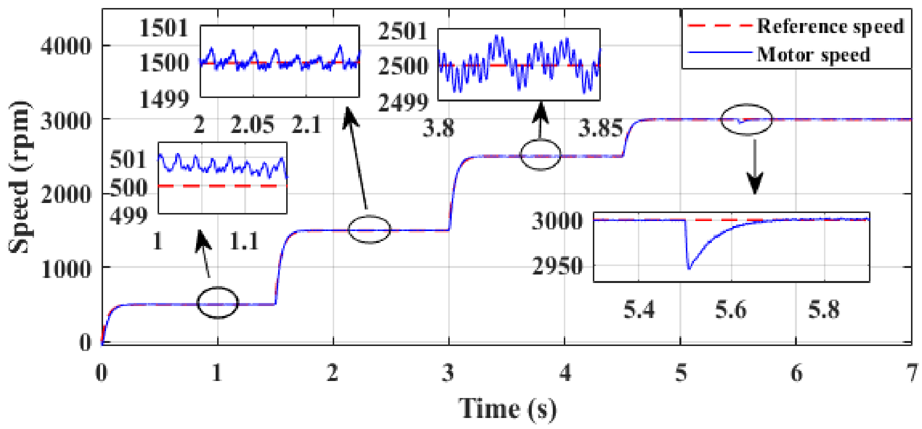

Fig. 9 The Motor Speed and Reference Speed.

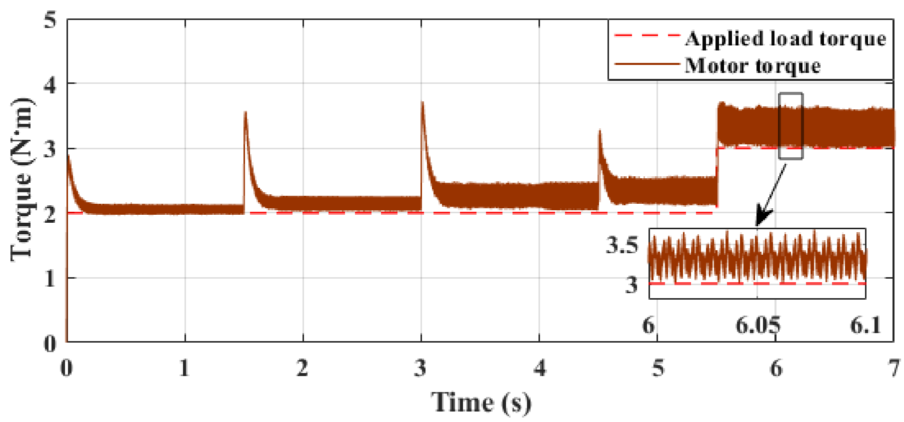

Fig. 10 The Applied Load Torque and Motor Torque.

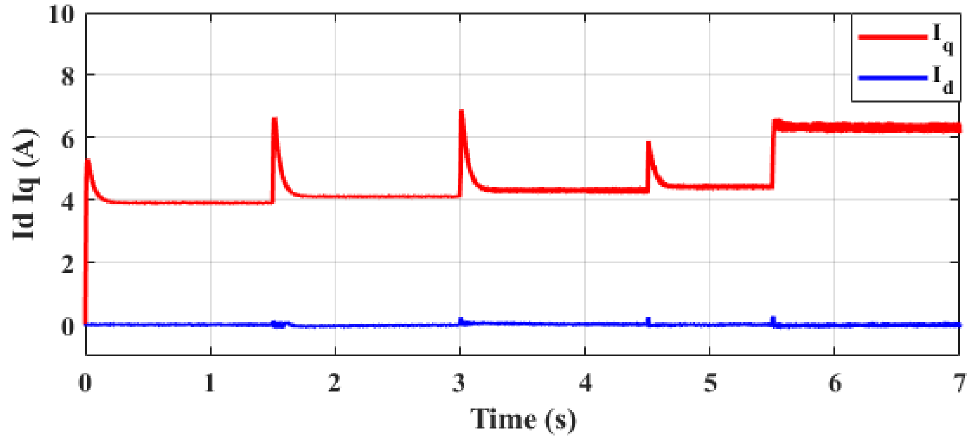

Fig. 11 I_d and I_q Current Components of the PMSM.

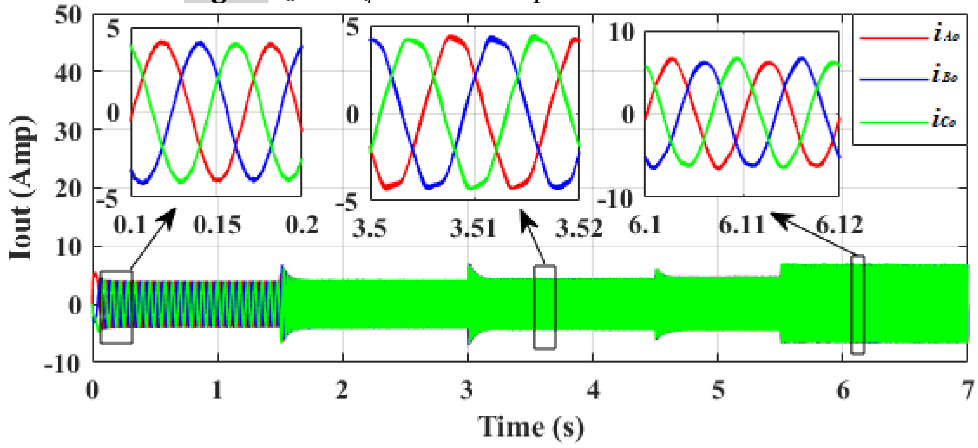

Fig. 12 PMSM Input Currents.

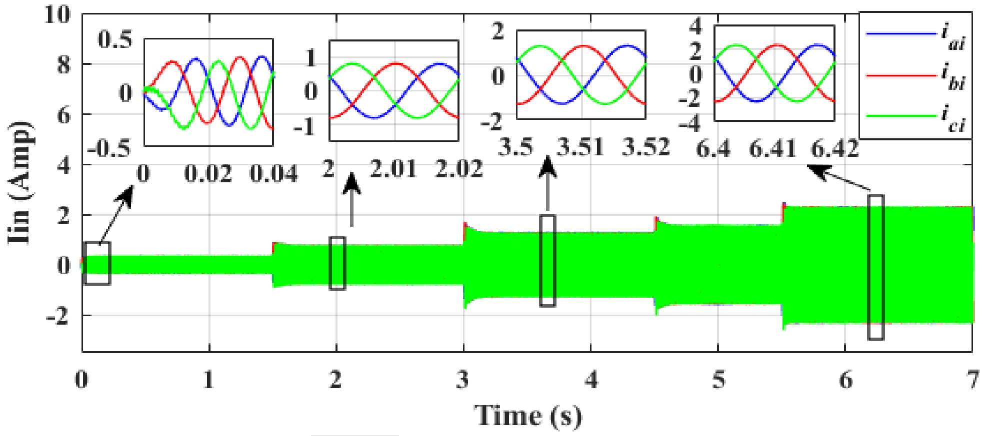

Fig. 13 Supply Input Currents.

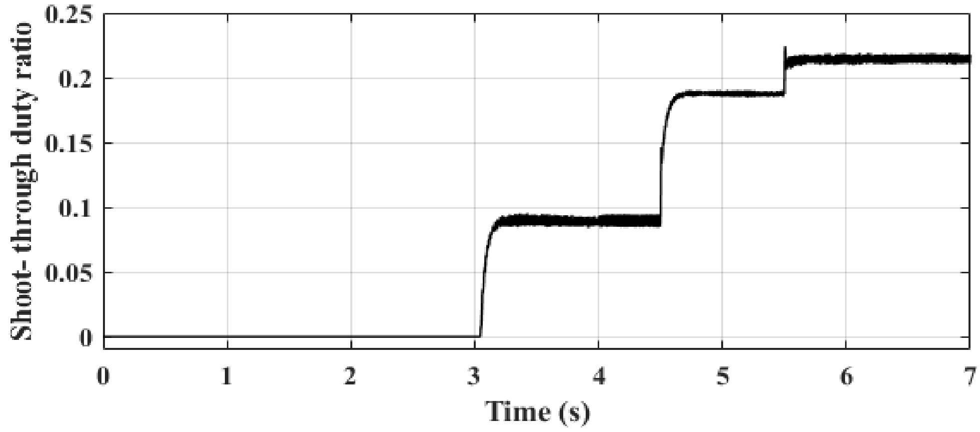

Fig. 14 Shoot-Through Duty Ratio.

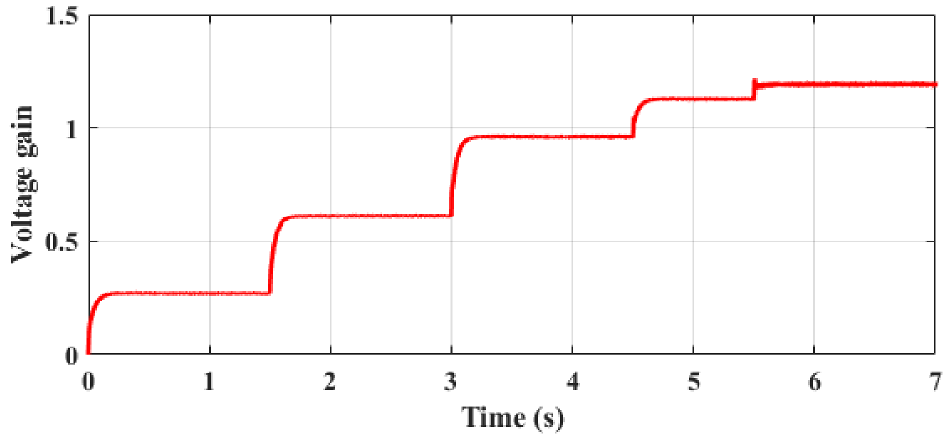

Fig. 15 Voltage Gain U_g.

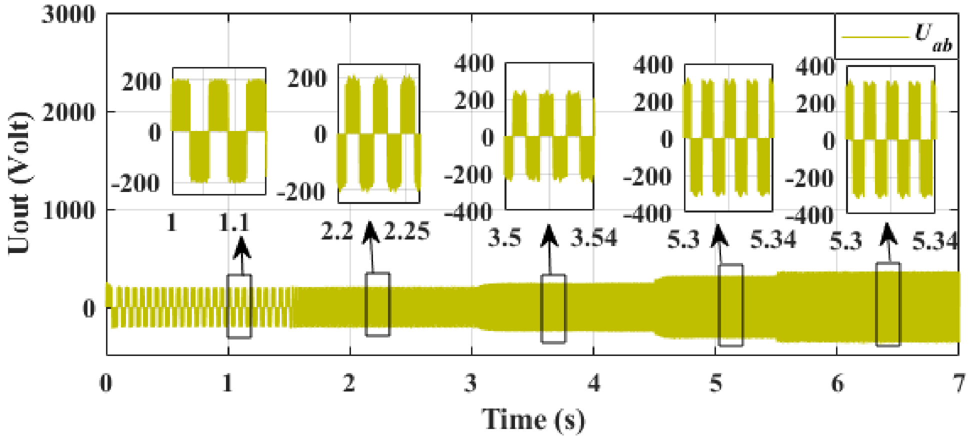

Fig. 16 Converter Output Voltages.

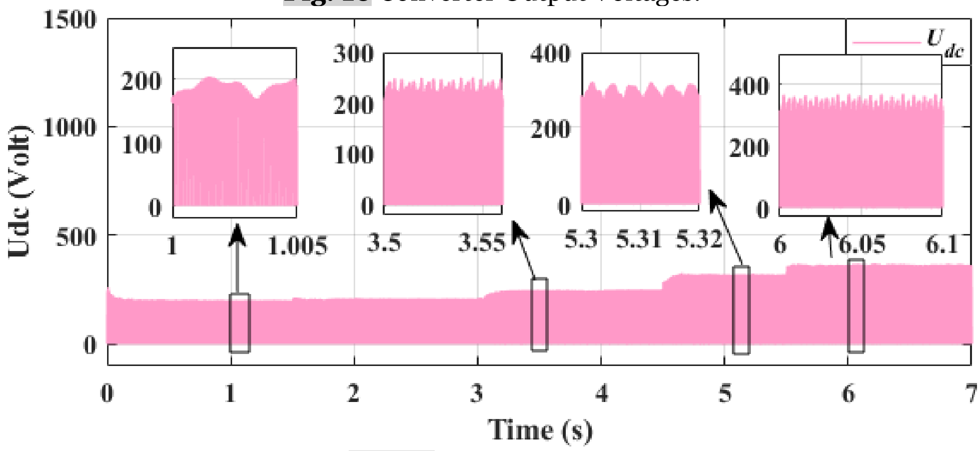

Fig. 17 DC-Bus Voltage.

7.2.State 2

In this state, the proposed converter operated with rated motor speed of 3000 rpm and applied load torque of 3 N·m with 100% and under 75% and 40% voltage sag supply voltage from 220/√3 V to 165/√3 V to 132/√3 V and return to its rated value through a period of (1.5, 3, and 4.5) second, respectively, to demonstrate that the system can automatically regulate output voltage by selecting the best D value, as shown in Fig. 18. Due to the supply voltage decrease, the voltage gain U_g increased to require the motor voltage gain from (1.2 to 1.52 for 75% voltage sag) and (1.52 to 1.8 for 40% voltage sag). Thus, the shoot-through duty ratio also increased, as shown in Figs. 19 and 20, respectively. Figure 21 shows how the DC-bus voltage was adjusted during a voltage sag to the required level based on the reference motor speed, and then returned to its original value while the voltage sag returned to its rated value. As shown in Fig. 22, the converter output voltage responded similarly to the DC-bus voltage. The motor speed was maintained at 3000 rpm when the supply voltage was reduced because the FOC regulated the output reference voltages to fit the set speed. However, the load torque ripple increased when the supply voltage decreased, as shown in Fig. 23. As the supply voltage decreased, the converter output current remained at the same value with THD by 3.12%, 4.92% and 5.74%, and 3.12%, respectively. However, the supply input current increased with THD by 3.4%, 5.3%, 6.23%, and 3.4%, respectively, as shown in Figs. 24 and 25, respectively.

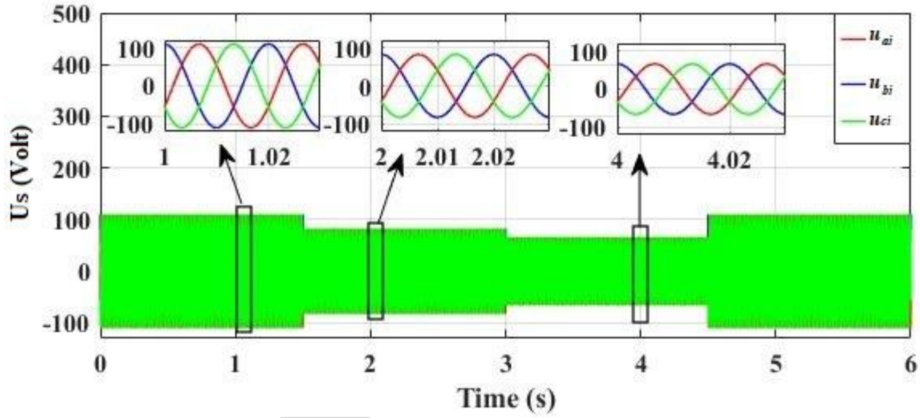

Fig. 18 Supply Input Voltages.

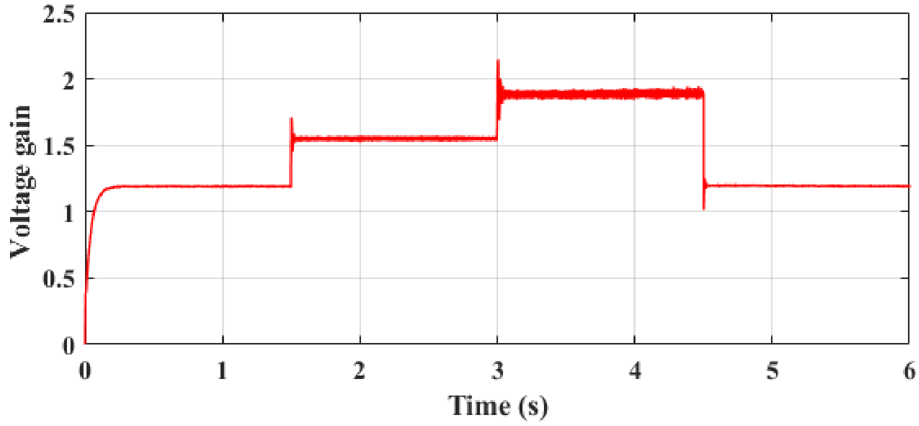

Fig. 19 Voltage Gain U_g.

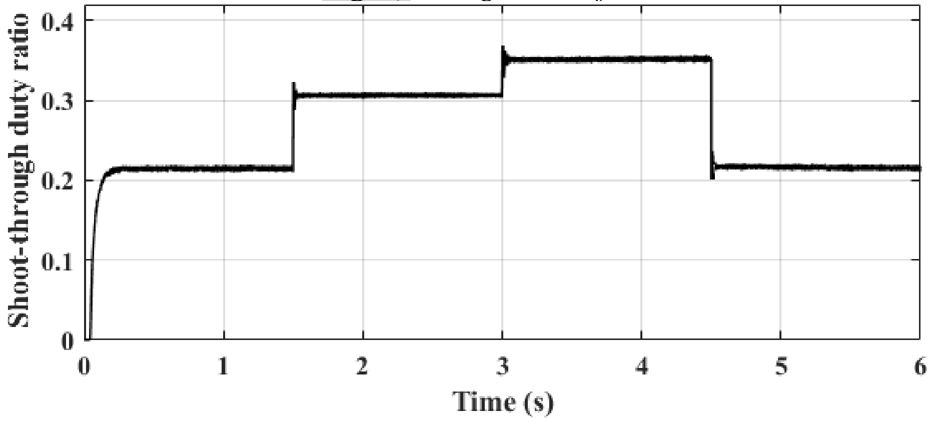

Fig. 20 Shoot-Through Duty Ratio.

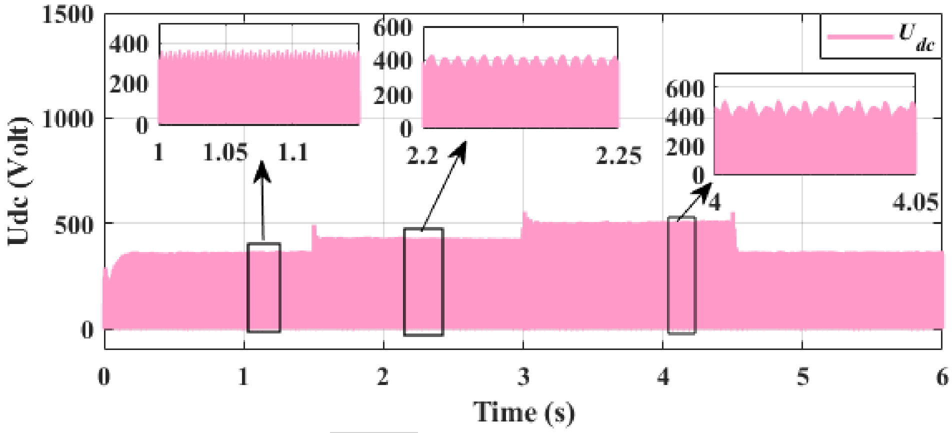

Fig. 21 DC-Bus Voltage.

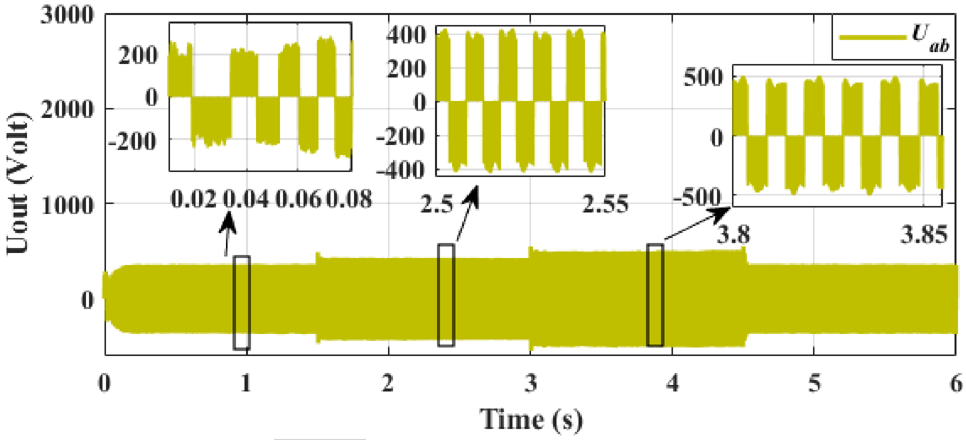

Fig. 22 Converter Output Voltages.

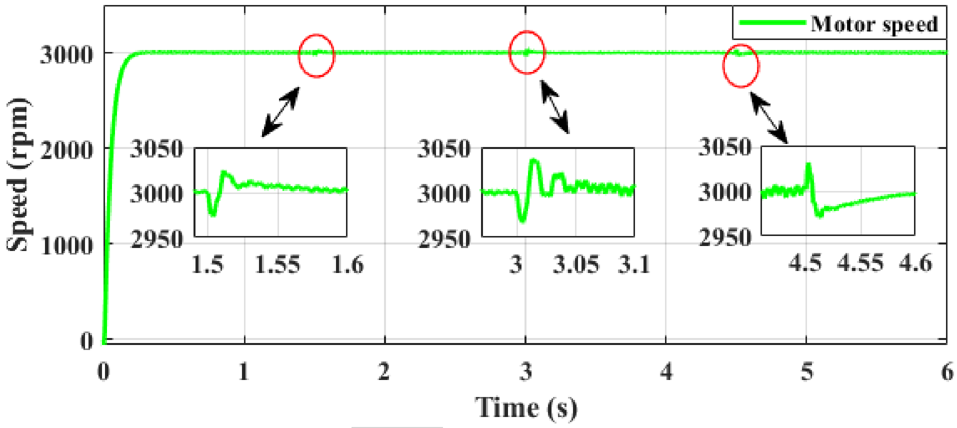

Fig. 23 Motor Speed.

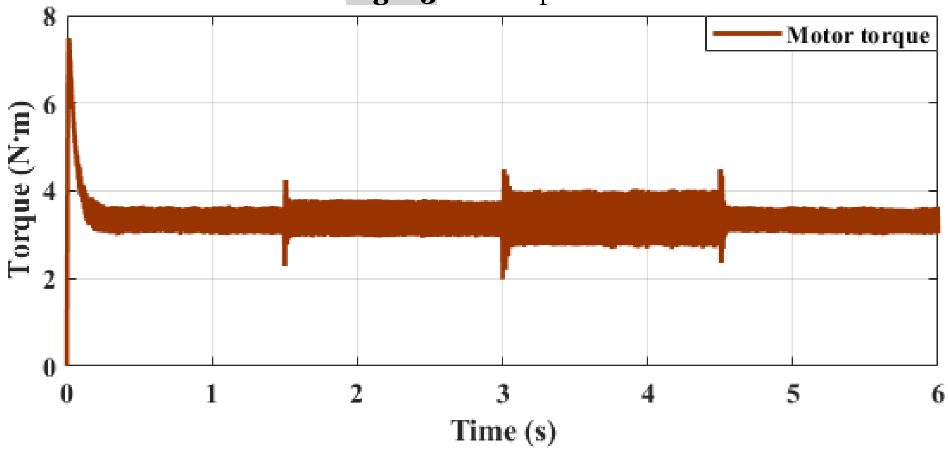

Fig. 24 Motor Load Torque.

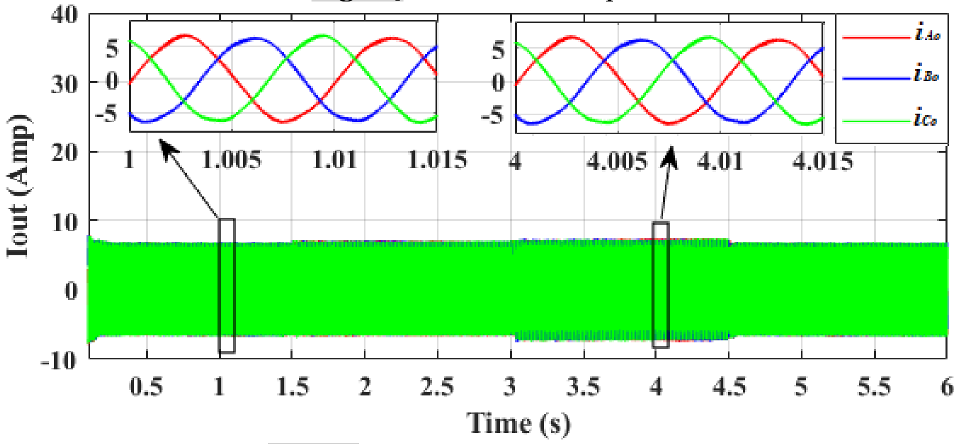

Fig. 25 Converter Output Currents.

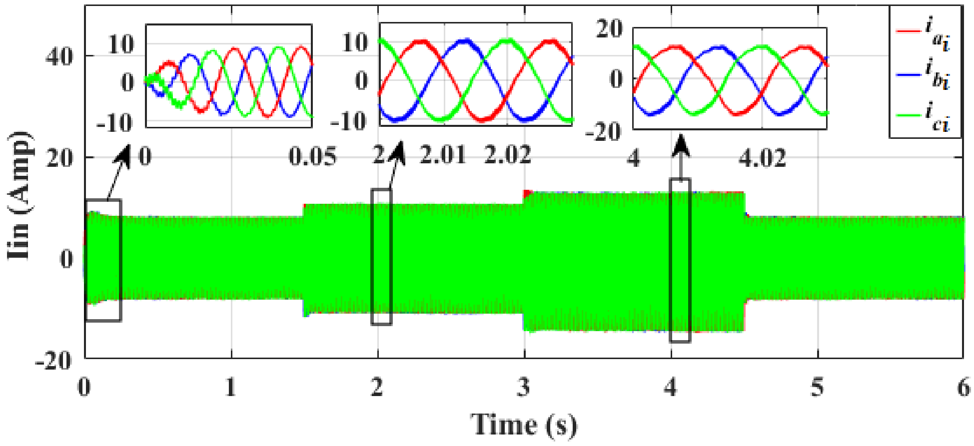

Fig. 26 Supply Input Currents.

8.CONCLUSIONS

The present paper proposes a quasi-Z-source IMC to drive a three-phase PMSM, as shown by the simulation results. The proposed quasi-Z-source IMC included all the capabilities of a traditional IMC in addition to its ability to boost voltage, allowing it to achieve a greater voltage gain than conventional converters. The voltage boost control strategy *D* was used to adjust the voltage gain of the quasi-Z-source IMC in response to changes in supply voltage, motor speed, and torque load. This action is also helpful for reducing the current and voltage stresses in the quasi-Z-source by choosing the best possible value for *D*. The input currents were in continuous mode, which means that the system did not need to add an input filter, reducing the size and cost of the converter.

REFERENCES

[1] Rao NT, Rao TL, Ashok G, Ponnada GN. **Modelling and Analysis of Matrix Converters Using MATLAB.** *IOP Conference Series: Earth and Environmental Science* 2024; **12028**.

[2] Kolar JW, Friedli T, Rodriguez J, Wheeler PW. **Review of Three-Phase PWM AC–AC Converter Topologies.** *IEEE Transactions on Industrial Electronics* 2011; **58**(11):4988-5006.

[3] Mohammed AM. **Study and Analysis of Multi-Pulse Converters in Modern Aircraft Electrical Power System.** *Tikrit Journal of Engineering Sciences* 2014; **21**(3):38-48.

[4] Nandhini E, Sivaprakasam A. **A Review of Various Control Strategies Based on Space Vector Pulse Width Modulation for the Voltage Source Inverter.** *IETE Journal of Research* 2022; **68**(5):3187-3201.

[5] Mahmood A, Gaeid K. **Review and Case Study on Control of Induction Motor Using High-Level Converter.** *Anbar Journal of Engineering Sciences* 2024; **15**(1):41-53.

[6] Jussila M, Tuusa H. **Comparison of Direct and Indirect Matrix Converters in Induction Motor Drive.** *IECON 2006-32nd Annual Conference on IEEE Industrial Electronics* 2006:1621-1626.

[7] Pipolo S, Formentini A, Trentin A, Zanchetta P, Calvini M, Venturini M. **A New Modulation Approach for Matrix Converter.** *2019 10th International Conference on Power Electronics and ECCE Asia* 2019:1021-1027.

[8] Guo M, Liu Y, Ge B, Liu S, Li X, Ferreira FJTE. **Modeling and Analysis of LC Filter Integrated Quasi-Z Source Indirect Matrix Converter.** *International Journal of Circuit Theory and Applications* 2020; **48**(4):567-586.

[9] Wheeler PW, Rodriguez J, Clare JC, Empringham L, Weinstein A. **Matrix Converters: A Technology Review.** *IEEE Transactions on Industrial Electronics* 2002; **49**(2):276-288.

[10] Bouazdia M, Bouhamida M, Taleb R, Denai M. **Performance Comparison of Field Oriented Control Based Permanent Magnet Synchronous Motor Fed by Matrix Converter Using PI and IP Speed Controllers.** *Indonesian Journal of Electrical Engineering and Computer Science* 2020; **19**(3):1156-1168.

[11] Friedli T, Kolar JW, Rodriguez J, Wheeler PW. **Comparative Evaluation of Three-Phase AC–AC Matrix Converter and Voltage DC-Link Back-to-Back Converter Systems.** *IEEE Transactions on Industrial Electronics* 2011; **59**(12):4487-4510.

[12] Empringham L, Kolar JW, Rodriguez J, Wheeler PW, Clare JC. **Technological Issues and Industrial Application of Matrix Converters: A Review.** *IEEE Transactions on Industrial Electronics* 2012; **60**(10):4260-4271.

[13] Vidhya DS, Venkatesan T. **Quasi-Z-Source Indirect Matrix Converter Fed Induction Motor Drive for Flow Control of Dye in Paper Mill.** *IEEE Transactions on Power Electronics* 2017; **33**(2):1476-1486.
[14] Guo M, Liu Y, Ge B, Li X, de Almeida AT, Ferreira FJTE. **Dual, Three-Level, Quasi-Z-Source, Indirect Matrix Converter for Motors with Open-Ended Windings.** *IEEE Transactions on Energy Conversion* 2022; **38**(1):64-74.
[15] Yoon Y-D, Sul S-K. **Carrier-Based Modulation Technique for Matrix Converter.** *IEEE Transactions on Power Electronics* 2006; **21**(6):1691-1703.
[16] Karaman E, Farasat M, Trzynadlowski AM. **A Comparative Study of Series and Cascaded Z-Source Matrix Converters.** *IEEE Transactions on Industrial Electronics* 2014; **61**(10):5164-5173.
[17] Maheswari KT, Kumar C, Balachandran PK, Senjyu T. **Modeling and Analysis of the LC Filter-Integrated Quasi Z-Source Indirect Matrix Converter for the Wind Energy Conversion System.** *Frontiers in Energy Research* 2023; **11**(August):1-16.
[18] Hameed SR, Al-Mhana TH. **Cascaded H–Bridge Multilevel Inverter: Review of Topologies and Pulse Width Modulation.** *Tikrit Journal of Engineering Sciences* 2024; **31**(1):138-151.
[19] Purwanto E, Murdianto FD, Wahyu Herlambang D, Basuki G, Jati MP. **Three-Phase Direct Matrix Converter with Space Vector Modulation for Induction Motor Drive.** *Proceedings of ICAITI 2019 - 2nd International Conference on Applied Information Technology and Innovation* 2019:11-16.
[20] Palanisamy R, Vijayakumar K, Selvabharathi D. **MSPWM Based Implementation of Novel 5-Level Inverter with Photovoltaic System.** *International Journal of Power Electronics and Drive Systems* 2017; **8**(4): 1494-1502.
[21] Sieklucki G, Sobieraj S, Gromba J, Necula R-E. **Analysis and Approximation of THD and Torque Ripple of Induction Motor for SVPWM Control of VSI.** *Energies* 2023; **16**(12): 4628.
[22] Sekhar CSA, Kumar RH, Rajan VRR, Sasikumar M. **Space Vector Modulation Based Direct Matrix Converter for Stand-Alone System.** *International Journal of Power Electronics and Drive Systems* 2014; **4**(1):24-32.
[23] Nayak B, Dash SS, Kumar S. **Proposed Method for Shoot-Through in Three Phase ZSI and Comparison of Different Control Techniques.** *International Journal of Power Electronics and Drive Systems* 2014; **5**(1):32-41.
[24] Sham NMB, Zulkifli SA, Jackson R. **i-Capacitor Voltage Control for PV Z-Source System with Enhanced Shoot-Through.** *International Journal of Power Electronics and Drive Systems* 2018; **9**(4):1899-1908.
[25] Rao MA. **FLC-MPC Based Direct Torque Control for Matrix Converter-Fed Induction Motor Drive.** *2015 International Renewable and Sustainable Energy Conference* 2015:1-6.
[26] Liu S, Ge B, Jiang X, Abu-Rub H, Peng F. **Modeling, Analysis, and Motor Drive Application of Quasi-Z-Source Indirect Matrix Converter.** *COMPEL: The International Journal for Computation and Mathematics in Electrical and Electronic Engineering* 2013; **33**(1/2):298-319.
[27] You X, Ge B, Liu S, Nie N, Jiang X, Abu-Rub H. **Common Mode Voltage Reduction of Quasi-Z Source Indirect Matrix Converter.** *International Journal of Circuit Theory and Applications* 2016; **44**(1):162-184.
[28] Liu S, Ge B, Jiang X, Abu-Rub H, Peng FZ. **Simplified Quasi-Z Source Indirect Matrix Converter.** *International Journal of Circuit Theory and Applications* 2015; **43**(11):1775-1793.
[29] Sudharani S, Nalini M. **Modeling of Single-Phase Matrix Converter Using MATLAB.** *International Journal of Advances in Engineering and Management* 2023; **5**(5):282-286.
[30] Ellabban O, Abu-Rub H, Ge B. **A Quasi-Z-Source Direct Matrix Converter Feeding a Vector Controlled Induction Motor Drive.** *IEEE Journal of Emerging and Selected Topics in Power Electronics* 2014; **3**(2):339-348.
[31] Hannan AK, Kadhum ZA, Ali AK, Farghly A, Hanan IK. **Suppression of the Capacitor Voltage Ripple in Modular Multilevel Converter for Variable-Speed Drive Applications.** *Tikrit Journal of Engineering Sciences* 2024; **31**(1):56-74.
[32] Hannan AK, Hassan TK. **Design and Simulation of Modular Multilevel Converter Fed Induction Motor Drive.** *Indonesian Journal of Electrical Engineering and Informatics* 2021; **9**(1):22-36.

[33] Es-saadi M, Khafallah M, Jammali M, Brik AA, Khoukh A, Chaikhy H. **Using the Five-Level NPC Inverter to Improve the FOC Control of the Asynchronous Machine.** *2017 International Renewable and Sustainable Energy Conference* 2017:1-6.

[34] Hammami R, Ameur I Ben, Jelassi K. **Performance Evaluation of Fractional Order Controller for Induction Machine Control and Comparative Study Between FOC PI and FOC FOPI.** *2017 18th International Conference on Sciences and Techniques of Automatic Control and Computer Engineering* 2017:272-277.

[35] Wahid S, Khammari H, Mimouni MF. **On Some Parametric and Phase Space Singularities in PMSM Submitted to FOC Drive.** *2015 7th International Conference on Modelling, Identification and Control* 2015:1-7.

[36] Khalid M, Mohan A. **Performance Analysis of Vector Controlled PMSM Drive Modulated with Sinusoidal PWM and Space Vector PWM.** *2020 IEEE International Power and Renewable Energy Conference* 2020:1-6.